

Search for $B^+ \rightarrow D^+ 0$ decay

M. Iwabuchi,⁴ M. Nakao,⁷ I. Adachi,⁷ K. Arinstein,¹ V. Aulchenko,¹ T. Aushev,^{16,11} A. M. Bakich,³⁶ V. Balagura,¹¹
 E. Barberio,¹⁹ A. Bay,¹⁶ K. Belous,¹⁰ V. Bhardwaj,³¹ U. Bitenc,¹² A. Bozek,²⁵ M. Bracko,^{18,12} T. E. Browder,⁶
 A. Chen,²² W. T. Chen,²² B. G. Cheon,⁵ I.-S. Cho,⁴⁵ Y. Choi,³⁵ J. Dalseno,⁷ M. Dash,⁴⁴ A. Dnutsyoy,³
 S. Eideman,¹ M. Fujikawa,²¹ N. Gabyshev,¹ H. Ha,¹⁴ J. Haba,⁷ K. Hayasaka,²⁰ M. Hazumi,⁷ D. Heeman,³⁰
 Y. Horii,³⁹ Y. Hoshi,³⁸ W.-S. Hou,²⁴ H. J. Hyun,¹⁵ K. Inami,²⁰ A. Ishikawa,³² H. Ishino,⁴¹ R. Itoh,⁷ M. Iwasaki,⁴⁰
 D. H. Kah,¹⁵ H. Kaji,²⁰ J. H. Kang,⁴⁵ H. Kawai,² T. Kawasaki,²⁷ H. Kichimi,⁷ H. J. Kim,¹⁵ H. O. Kim,¹⁵
 Y. I. Kim,¹⁵ Y. J. Kim,⁴ K. Kinoshita,³ S. Korpar,^{18,12} P. Krizan,^{17,12} P. Rokovny,⁷ R. Kumar,³¹ C. C. Kuo,²²
 Y.-J. Kwon,⁴⁵ J. S. Lee,³⁵ M. J. Lee,³⁴ S. E. Lee,³⁴ T. Lesiak,²⁵ A. Limosani,¹⁹ S.-W. Lin,²⁴ C. Liu,³³ Y. Liu,⁴
 D. Liventsev,¹¹ F. Mandl,⁹ A. Matyjka,²⁵ S. M. Mironov,³⁶ T. M. Medvedeva,¹¹ K. Miyabayashi,²¹ H. Miyake,³⁰
 H. Miyata,²⁷ Y. Miyazaki,²⁰ G. R. M. Olney,¹⁹ H. Nakazawa,²² Z. Natkaniec,²⁵ S. Nishida,⁷ O. Nito,⁴³ S. Ogawa,³⁷
 T. Ohshima,²⁰ S. Okuno,¹³ H. Ozaki,⁷ P. Pakhlov,¹¹ G. Pakhlova,¹¹ C. W. Park,³⁵ H. K. Park,¹⁵ K. S. Park,³⁵
 L. S. Peak,³⁶ R. Pestotnik,¹² L. E. Piihonen,⁴⁴ H. Sahoo,⁶ Y. Sakai,⁷ O. Schneider,¹⁶ J. Schumann,⁷ C. Schwanda,⁹
 A. Sekiya,²¹ K. Senyo,²⁰ M. Shapkin,¹⁰ H. Shibuya,³⁷ J.-G. Shiu,²⁴ B. Schwartz,¹ S. Stanic,²⁸ M. Starić,¹²
 K. Sumisawa,⁷ T. Sumiyoshi,⁴² S. Suzuki,³² M. Tanaka,⁷ Y. Teramoto,²⁹ I. Tikhonov,¹¹ K. Trabelsi,⁷
 Y. Uchida,⁴ S. Uehara,⁷ T. Uglav,¹¹ Y. Unno,⁵ S. Uno,⁷ P. Urquijo,¹⁹ Y. Usov,¹ G. Vamer,⁶ K. E. Varvell,³⁶
 K. Vervink,¹⁶ C. C. Wang,²⁴ C. H. Wang,²³ M.-Z. Wang,²⁴ P. Wang,⁸ X. L. Wang,⁸ Y. Watanabe,¹³
 J. Wicht,¹⁶ E. Won,¹⁴ Y. Yamashita,²⁶ Z. P. Zhang,³³ V. Zhilich,¹ V. Zhulanov,¹ and A. Zupanc¹²

(The Belle Collaboration)

¹Budker Institute of Nuclear Physics, Novosibirsk

²Chiba University, Chiba

³University of Cincinnati, Cincinnati, Ohio 45221

⁴The Graduate University for Advanced Studies, Hayama

⁵Hanyang University, Seoul

⁶University of Hawaii, Honolulu, Hawaii 96822

⁷High Energy Accelerator Research Organization (KEK), Tsukuba

⁸Institute of High Energy Physics, Chinese Academy of Sciences, Beijing

⁹Institute of High Energy Physics, Vienna

¹⁰Institute of High Energy Physics, Protvino

¹¹Institute for Theoretical and Experimental Physics, Moscow

¹²J. Stefan Institute, Ljubljana

¹³Kanagawa University, Yokohama

¹⁴Korea University, Seoul

¹⁵Kyungpook National University, Taegu

¹⁶Ecole Polytechnique Fédérale de Lausanne (EPFL), Lausanne

¹⁷Faculty of Mathematics and Physics, University of Ljubljana, Ljubljana

¹⁸University of Maribor, Maribor

¹⁹University of Melbourne, School of Physics, Victoria 3010

²⁰Nagoya University, Nagoya

²¹Nara Women's University, Nara

²²National Central University, Chung-li

²³National United University, Miaoli

²⁴Department of Physics, National Taiwan University, Taipei

²⁵H. Niewodniczanski Institute of Nuclear Physics, Krakow

²⁶Niigata Dental University, Niigata

²⁷Niigata University, Niigata

²⁸University of Nova Gorica, Nova Gorica

²⁹Osaka City University, Osaka

³⁰Osaka University, Osaka

³¹Punjab University, Chandigarh

³²Saga University, Saga

³³University of Science and Technology of China, Hefei

³⁴Seoul National University, Seoul

³⁵Sungkyunkwan University, Suwon

³⁶University of Sydney, Sydney, New South Wales

³⁷Toho University, Funabashi

³⁸Tohoku Gakuin University, Tagajo

³⁹Tohoku University, Sendai

⁴⁰Department of Physics, University of Tokyo, Tokyo

⁴¹Tokyo Institute of Technology, Tokyo

⁴²Tokyo Metropolitan University, Tokyo

⁴³Tokyo University of Agriculture and Technology, Tokyo

⁴⁴Virginia Polytechnic Institute and State University, Blacksburg, Virginia 24061

⁴⁵Yonsei University, Seoul

We report on a search for the doubly Cabibbo suppressed decay $B^+ \rightarrow D^+ \pi^0$, based on a data sample of $657 \times 10^6 B\bar{B}$ pairs collected at the $(4S)$ resonance with the Belle detector at the KEKB asymmetric energy e^+e^- collider. We find no significant signal and set an upper limit of $B(B^+ \rightarrow D^+ \pi^0) < 3.6 \times 10^{-6}$ at the 90% confidence level. This limit can be used to constrain the ratio between suppressed and favored $B \rightarrow D$ decay amplitudes, $r < 0.051$, at the 90% confidence level.

PACS numbers: 11.30.Er, 12.15.Hh, 13.25.Hw, 14.40.Nd

In the Standard Model, CP violation arises from a complex phase in the Cabibbo-Kobayashi-Maskawa (CKM) quark mixing matrix [1, 2]. Precise measurements of CKM matrix parameters are therefore of fundamental importance for the description of the weak interaction of quarks and the investigation for the new sources of CP violation. Measurements of the time-dependent decay rates of $B^0 \rightarrow D^+ D^-$ provide a theoretically clean method for extracting $\sin(2\alpha_1 + \alpha_3)$ [3], where α_1 and α_3 are the interior angles of the CKM triangle [4]. The CP violation parameters S are given by [5]

$$S = \frac{2(1+r)\sin(2\alpha_1 + \alpha_3)}{1+r^2}; \quad (1)$$

where r is the ratio of the amplitudes of the doubly Cabibbo suppressed decay (DCSD), $B^0 \rightarrow D^+ D^-$ to the Cabibbo favored decay (CFD), $B^0 \rightarrow D^+ D^-$ (Fig. 1), L denotes the angular momentum of the final state, and δ is the strong phase difference between DCSD and CFD. It is difficult to determine r from B^0 decays because the DCSD amplitude is small compared to the contribution from mixing followed by CFD, $B^0 \rightarrow \bar{B}^0 \rightarrow D^+ D^-$.

Using available branching fraction measurements, r can be written in the following expression,

$$r = \tan \theta_c \frac{f_D}{f_{D_s}} \frac{S(B^0 \rightarrow D_s^+ D^-)}{S(B^0 \rightarrow D^+ D^-)}; \quad (2)$$

where θ_c is the Cabibbo angle, and the decay constants f_D and f_{D_s} are available from lattice QCD calculations. However, the assumption of SU(3) symmetry and additional W -exchange contributions result in an uncertainty of about 30% on r . In order to avoid this uncertainty, one can instead use the isospin relation,

$$r = \frac{S(B^0 \rightarrow 2B^+ \rightarrow D^+ D^-)}{S(B^+ \rightarrow B^0 \rightarrow D^+ D^-)}; \quad (3)$$

where $B^+ = B^0 = 1.071 \pm 0.009$ and $B(B^0 \rightarrow D^+ D^-) = (2.76 \pm 0.21) \times 10^{-3}$ [6]. We naively estimate $B(B^+ \rightarrow D^+ \pi^0) = 5.9 \times 10^{-7}$, taking into account the r factor of 0.02 calculated from Eq. (2) [7].

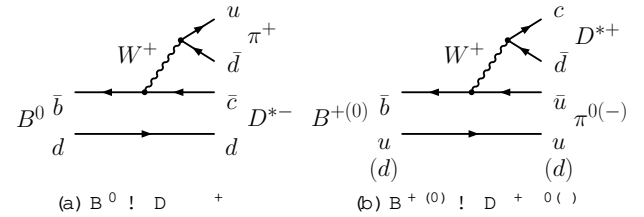


FIG. 1: Feynman tree diagrams for (a) CFD $B^0 \rightarrow D^+ \pi^0$ with the CKM coupling $V_{cb}V_{ud}$, and (b) DCSD $B^+ \rightarrow D^+ \pi^0$ with the coupling $V_{ub}V_{cd}$.

In this Letter, we report on a search for $B^+ \rightarrow D^+ \pi^0$ based on a data sample of 605 fb^{-1} corresponding to $(657 \pm 9) \times 10^6 B\bar{B}$ events, collected with the Belle detector [8] at the KEKB asymmetric-energy e^+e^- collider [9] operating at the $(4S)$ resonance.

The Belle detector is a large-solid-angle magnetic spectrometer that consists of a silicon vertex detector, a 50-layer central drift chamber (CDC), an array of aerogel threshold Cherenkov counters (ACC), a barrel-like arrangement of time-of-flight scintillation counters (TOF), and an electromagnetic calorimeter comprised of CsI(Tl) crystals located inside a superconducting solenoid coil that provides a 1.5 T magnetic field. An iron flux-return located outside of the coil is instrumented to detect K_L^0 mesons and to identify muons.

To search for $B^+ \rightarrow D^+ \pi^0$, we reconstruct D^+ candidates by pairing a low momentum charged pion (π_{slow}^+) and a D^0 , which is reconstructed through its decays to K^+ , $K^+ \pi^0$, $K^+ \eta$ and $K_S^0 \pi^+$. Inclusion of charge conjugate modes is implied throughout this Letter.

For charged kaon and pion candidates except pions

from K_S^0 's, we require tracks to have a distance of closest approach to the interaction point within 5 cm along the z-axis (anti-parallel to the positron beam direction) and within 2 cm in a plane perpendicular to the z-axis. Particle identification (PID) is based on the likelihoods $R(K^\pm) = L_K = (L_K + L_\pi)$, where $L_K = L_\pi$ is the likelihood of kaons/pions derived from the TOF, ACC and dE/dx measurements in the CDC. The PID selections, which are $R(K^\pm) > 0.3$ (< 0.3) for kaons (pions) are applied to all charged particles except pions from K_S^0 's. The PID efficiencies are 94% (91%) for kaons (pions), while the probability of misidentifying a pion as a kaon (a kaon as a pion) is 12% (6%).

Neutral pions are formed from photon pairs with an invariant mass between $0.118 \text{ GeV} = c^2$ and $0.150 \text{ GeV} = c^2$, corresponding to ± 3 standard deviations (σ). The photon momenta are then recalculated with a 0 mass constraint. We require the 0 momentum to be greater than $0.2 \text{ GeV} = c$ in the center-of-mass system (cms), and the photon energy to be greater than 0.1 GeV in the laboratory frame.

K_S^0 candidates are reconstructed from pion pairs of oppositely-charged tracks with an invariant mass between $0.485 \text{ GeV} = c^2$ and $0.510 \text{ GeV} = c^2$, corresponding to $\pm 5\sigma$. Each candidate must have a displaced vertex with a flight direction consistent with that of a K_S^0 meson originating from the interaction point. Mass- and vertex-constrained fits are applied to obtain the 4-momenta of K_S^0 candidates.

For D^0 selection, the invariant mass of the daughter particles is required to be within 3σ from the nominal D^0 mass, where $\sigma = 5 \text{ MeV} = c^2$ depends on the decay mode. D^+ candidates are required to have a mass difference $M = M_D - M_{D^+}$ within 3σ from the nominal mass difference, where $\sigma = 0.5 \text{ MeV} = c^2$ depends on the decay mode. Mass- and vertex-constrained fits are applied to D^0 and D^+ candidates.

We reconstruct a B^+ candidate from a D^+ and a 0 candidate. We identify B decays based on requirements on the energy difference $E = E_{D^+} - E_{0}$, E_{beam} and the beam-energy constrained mass $M_{bc} = \sqrt{E_{\text{beam}}^2 - \sum_i \vec{p}_i^2}$, where E_{beam} is the beam energy, and \vec{p}_i and E_i are the momenta and energies of the daughters of the reconstructed B meson candidate, all in the cms. We select candidates in a t region defined as $j E_j < 0.25 \text{ GeV}$ and $5.20 \text{ GeV} = c^2 < M_{bc} < 5.29 \text{ GeV} = c^2$. The signal region is defined as $j E_j < 0.1 \text{ GeV}$ and $5.27 \text{ GeV} = c^2 < M_{bc} < 5.29 \text{ GeV} = c^2$.

To suppress the background from continuum ($e^+e^- \rightarrow q\bar{q}$; $q = u; d; s; c$) events, we calculate modified Fox-Wolfram moments [10] and combine them into a Fisher discriminant. We calculate a probability density function (PDF) for this discriminant and multiply it by PDFs for $\cos \theta_B$, z and $\cos \theta_h$, where θ_B is the polar angle between the B direction and the beam direction in the cms, z is the displacement along the beam axis be-

tween the signal B vertex and that of the other B, and θ_h is the angle between the $+$ direction and the opposite of the B momentum in the D^+ frame. The PDFs for signal, generic B events and continuum are obtained from GEANT3-based [11] Monte Carlo (MC) simulation. These PDFs are combined into a signal (background) likelihood variable $L_{\text{sig}(bkg)}$; we then impose requirements on the likelihood ratio $R = L_{\text{sig}} / (L_{\text{sig}} + L_{bkg})$. An additional background suppression is achieved through the use of a B-avor tagging algorithm [12], which provides a discrete variable indicating the flavor of the tagging B meson and a quality parameter r , with continuous values ranging from 0 for no flavor information to unity for unambiguous flavor assignment. The backgrounds from continuum and generic B events are reduced by applying a selection requirement on R for events in each r region that maximizes the value of $N_{\text{sig}} = N_{\text{sig}} + N_{bkg}$, where N_{sig} and N_{bkg} denote the expected signal and background yields in the signal region, based on MC simulation. This requirement eliminates 99% (94%) of the background from continuum (B decays) in the signal region, while retaining 35% of the signal.

The fraction of events with more than one candidate is 3%. We select the best D^+ candidate based on the value of $\chi^2_{\text{tot}} = \chi^2_{M(D^0)} + \chi^2_M + \chi^2_{M(0)}$, where each χ^2 is defined as the squared ratio of the deviation of the measured parameter from the expected signal value and the corresponding resolution. The signal efficiency in the signal region is estimated to be 0.56% from MC, which includes the D^+ and D^0 branching fractions [6].

After the selection criteria are applied, the dominant background sources in the t region are the continuum events and $\bar{B}^0 \rightarrow D^+$, while other B decays such as $B \rightarrow D^0$ and $\bar{B}^0 \rightarrow D^0$ have smaller contributions. To obtain the signal yield, we perform an unbinned two-dimensional (2D) extended maximum-likelihood fit to the $E - M_{bc}$ distributions in the t region. The likelihood function consists of the following components: signal, continuum background ($q\bar{q}$), $\bar{B}^0 \rightarrow D^+$ and other B decays.

The likelihood function for the signal is defined separately for each of the four D^0 decay modes and unified using the available branching fractions of the D^0 sub-decays [6], while those for $q\bar{q}$ and backgrounds from B decays are defined as the sum of four D^0 decay modes.

Each E and M_{bc} shape for the signal is modeled by the sum of a Gaussian and a bifurcated Gaussian with means and widths fixed to the values obtained from MC. The E and M_{bc} PDFs for $q\bar{q}$ are modeled by a linear function and an ARGUS function [13], respectively. The backgrounds from $\bar{B}^0 \rightarrow D^+$ and other B decays are modeled by the superposition of Gaussian distributions constructed from unbinned MC events, where the width of each Gaussian represents the smearing parameter for the event [14]. The $\bar{B}^0 \rightarrow D^+$ background forms a large peak in the region $E < 0.1 \text{ GeV}$ and

$5.27 \text{ GeV} = c^2 < M_{bc} < 5.29 \text{ GeV} = c^2$. The size and shape of the $\bar{B}^0 \rightarrow D^+$ component strongly depends on its helicity composition. We use the helicity amplitudes $(\mathcal{H}_0; \mathcal{H}_\parallel; \mathcal{H}_\perp) = (0.941; 0.322; 0.107)$ taken from Ref. [15].

The following parameters are allowed to vary in our fit to data: $q\bar{q}$ PDF parameters and yields of signal, $q\bar{q}$ and $\bar{B}^0 \rightarrow D^+$ components. The yield of other B decays is fixed to the branching fractions in Ref. [6].

Figure 2 shows the results of the fit to the data in the fit region. The projections of the fitted B signal in $E(M_{bc})$ in the $M_{bc}(E)$ signal region are shown. We obtain $4.5^{+4.1}_{-3.4} B^+ \rightarrow D^+ \pi^0$ signal candidates in the signal region with a statistical significance of 1.4, defined by $\sqrt{2 \ln(L_0/L_{\text{max}})}$ where L_0 and L_{max} are the likelihoods with the signal fixed to zero and at the fitted value, respectively.

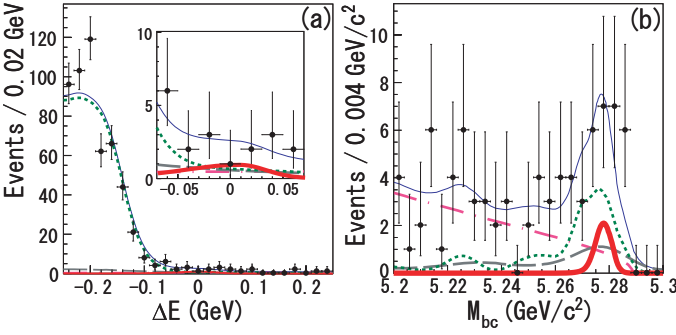


FIG. 2: Projections of the unbinned two-dimensional likelihood fit to data in the region $|E_j| < 0.25 \text{ GeV}$ and $5.20 \text{ GeV} = c^2 < M_{bc} < 5.29 \text{ GeV} = c^2$. (a) E distribution for $5.27 \text{ GeV} = c^2 < M_{bc} < 5.29 \text{ GeV} = c^2$ with a magnified view of $|E_j| < 0.07 \text{ GeV}$ in the inset. (b) M_{bc} distribution for $|E_j| < 0.1 \text{ GeV}$. The points with error bars represent the data, while the curves represent the various components from the fit: signal (thick solid), continuum (dash-dotted), $\bar{B}^0 \rightarrow D^+$ decay (dotted), other B decays (dashed), and the sum of all components (thin solid).

The systematic error components proportional to the signal yield are determined as follows. We estimate the systematic error from the R requirement by applying the R requirement to data and MC using a $B^+ \rightarrow D^0 \pi^+$ control sample. The systematic error on the M requirement is estimated by applying the M requirement to $\bar{B}^0 \rightarrow D^+$ data and $B^+ \rightarrow D^+ \pi^0$ MC. The systematic error on the secondary branching fraction is calculated from errors given in Ref. [6]. The systematic error due to the charged-track reconstruction efficiency is estimated to be 1.0% (1.6%) per charged kaon (pion) using partially reconstructed D^+ events. The systematic error due to R ($K = \pi$) selection has a relative uncertainty of 0.8% (1.4%) per charged kaon (pion), determined from

$D^+ \rightarrow D^0 \pi^+, D^0 \rightarrow K^+ \pi^0$ decays. The D^0 reconstruction is verified by comparing the ratio of $D^0 \rightarrow K^+ \pi^0$ and $D^0 \rightarrow K^+ \pi^0$ yields with the MC expectation; an uncertainty of 3.0% per particle is assigned. The K_S^0 reconstruction is verified by comparing the ratio of $D^+ \rightarrow K_S^0 \pi^+$ and $D^+ \rightarrow K^+ \pi^+$ yields with the MC expectation; an uncertainty of 4.9% is assigned. The systematic error due to signal MC statistics is 0.5% and the error due to the uncertainty in the total number of $B\bar{B}$ pairs is 1.4%. The systematic error components proportional to the signal yield are summarized in Table I.

The systematic errors on the yield extraction are estimated as follows. We estimate the uncertainty of \mathcal{H}_0 of $\bar{B}^0 \rightarrow D^+$ by varying \mathcal{H}_0 by ± 1 , where the error of \mathcal{H}_0 is taken from Ref. [15]. Possible E shifts between data and MC for the $\bar{B}^0 \rightarrow D^+$ background are evaluated by measuring the E shift of the $B^+ \rightarrow D^0 \pi^+$ background component using a $\bar{B}^0 \rightarrow D^0 \pi^0$ control sample. To obtain the systematic error on the background fraction of other B decays, we vary the normalizations of the individual sources by ± 1 , where the values are taken from Ref. [6]. The normalization of other background components are varied by $\pm 50\%$. The systematic error due to the uncertainty in the shape of the B background PDF is determined by varying the Gaussian smoothing width by factors of two and one half from its nominal value. Uncertainties from the two-dimensional correlation in the signal and the $q\bar{q}$ components are estimated by applying 2D background PDFs to the signal and the $q\bar{q}$ shapes. The effect of a possible bias in the fitting procedure is estimated by a toy MC study. The systematic errors on the yield extraction in the signal region are summarized in Table II.

TABLE I: Systematic errors for $B(B^+ \rightarrow D^+ \pi^0)$, proportional to the signal yield.

Source	Systematic error (%)
R requirement	3.0
M requirement	3.3
Secondary branching fractions	3.3
Track finding efficiency	5.1
Particle identification	4.4
D^0 reconstruction	4.1
K_S^0 reconstruction	0.3
MC statistics	0.5
Number of $B\bar{B}$ pairs	1.4
Quadratic sum	9.8

A likelihood distribution (L), which is convolved with an asymmetric Gaussian distribution that represents the systematic error, is used to obtain the upper limit on the branching fraction.

We calculate the 90% confidence level (CL) upper limit

TABLE II: Systematic errors for $B(B^+ \rightarrow D^+ \bar{D}^0)$, related to the yield extraction in the signal region.

Source	Systematic error (number of events)	
	+	
Model of $B^0 \rightarrow D^+ \bar{D}^0$	0.7	1.9
Shift of $B^0 \rightarrow D^+ \bar{D}^0$	0.0	0.6
Fraction of backgrounds	0.8	0.4
Gaussian width of background PDF	0.5	2.0
2D correlation for $q\bar{q}$ and $B^+ \rightarrow D^+ \bar{D}^0$	0.0	1.3
Fit bias	0.0	0.5
Quadratic sum	1.2	3.2

(UL) using the relation $R_{UL} = R_1 = 0.9$ to be

$$B(B^+ \rightarrow D^+ \bar{D}^0) < 3.6 \times 10^{-6}: \quad (4)$$

The obtained upper limit is consistent with the naive estimate, 5.9×10^{-7} discussed above.

This result can be used to obtain an upper limit on the ratio of magnitudes of DCS and CF in D decay,

$$r < 0.051 \text{ (90\% CL)}: \quad (5)$$

To summarize, a search for the doubly Cabibbo suppressed decay $B^+ \rightarrow D^+ \bar{D}^0$ in a data sample of 605 fb^{-1} , yields an upper limit of $B(B^+ \rightarrow D^+ \bar{D}^0) < 3.6 \times 10^{-6}$ at the 90% confidence level. This limit can be used to constrain the ratio between suppressed and favored $B \rightarrow D$ decay amplitudes, $r < 0.051$, at the 90% confidence level.

We thank the KEKB group for excellent operation of the accelerator, the KEK cryogenics group for efficient solenoid operations, and the KEK computer group and the NII for valuable computing and SINET3 network support. We acknowledge support from MEXT

and JSPS (Japan); ARC and DEST (Australia); NSFC (China); DST (India); MOEHRD, KOSEF and KRF (Korea); KBN (Poland); MES and RFAAE (Russia); ARRS (Slovenia); SNSF (Switzerland); NSC and MOE (Taiwan); and DOE (USA).

- [1] N. Cabibbo, Phys. Rev. Lett. 10, 531 (1963).
- [2] M. Kobayashi and T. Maskawa, Prog. Theor. Phys. 49, 652 (1973).
- [3] I. Dunietz and R. G. Sachs, Phys. Rev. D 37, 3186 (1988); Erratum ibid. 39, 3515 (1989); I. Dunietz, Phys. Lett. B 427, 179 (1998).
- [4] The angles α_1 and α_3 are also sometimes known as α and β , respectively.
- [5] R. Fleischer, Nucl. Phys. B 671, 459 (2003).
- [6] Y.-M. Yao et al. (Particle Data Group), J. Phys. G 33, 1 (2006).
- [7] F. J. Ronga and T. R. Sarangi et al. (Belle Collaboration), Phys. Rev. D 73, 092003 (2006).
- [8] A. Abashian et al. (Belle Collaboration), Nucl. Instr. and Meth. A 479, 117 (2002).
- [9] S. Kurokawa and E. Kikutani, Nucl. Instr. and Meth. A 499, 1 (2003), and other papers included in this volume.
- [10] G. C. Fox and S. Wolfram, Phys. Rev. Lett. 41, 1581 (1978). The modified moments used in this Letter are described in, S. H. Lee et al. (Belle Collaboration), Phys. Rev. Lett. 91, 261801 (2003).
- [11] R. Brun et al., GEANT 3.21, CERN Report DD/EE/84-1 (1984).
- [12] H. Kakuno et al., Nucl. Instr. and Meth. A 533, 516 (2004).
- [13] H. Albrecht et al. (ARGUS Collaboration), Phys. Lett. B 241, 278 (1990).
- [14] K. Cranmer, Comput. Phys. Commun. 136, 198 (2001).
- [15] S. E. Csoma et al. (CLEO Collaboration), Phys. Rev. D 67, 112002 (2003).